UNIVERSITY OF PADOVA
Department of Civil, Environmental and Architectural Engineering – DICEA
Department of Management and Engineering – DTG

GEOMETRICAL RECONSTRUCTION OF CONCRETE MATERIALS THROUGH THE AID OF ADVANCED MEASUREMENT TECHNIQUES AND STUDIES OF THEIR MECHANICAL BEHAVIOR

G. Mazzucco*, G. Xotta, B. Pomaro, V.A. Salomoni, C.E. Majorana

INTRODUCTION

- EAF (Electric Arc Furnace) concrete shows an improved compressive and tensile strength due to the slag morphology and shape, which is found to enhance the adherence with the cementitious matrix.

- The elastic modulus of EAF concrete is generally higher than conventional concrete → the replacement of coarse natural aggregates with EAF slag allows to design high-strength concretes maintaining relative high w/c ratios (around 0.4-0.5).

- The main application in Europe is the bank reinforcement and ground improvement of harbor sites.

- EAF concrete has generally comparable specific weight to baritic concrete, consequently it shows similar shielding capacity of a heavy-weight concrete against nuclear radiation.

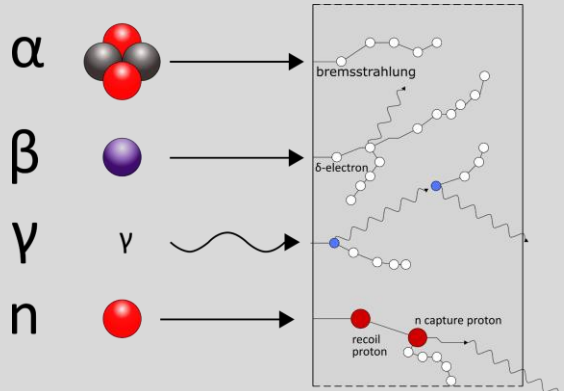

INTRODUCTION

- It is known that concrete with different confinement levels presents different mechanical responses.

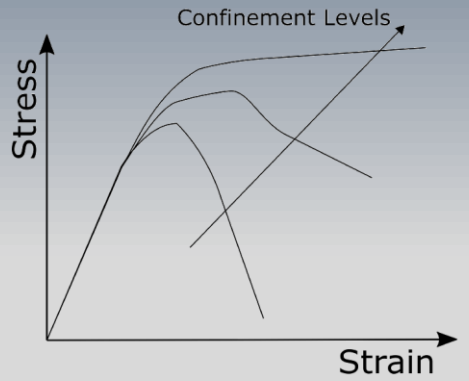

- In a meso-scale approach the presence of aggregates implies a local confinement effect (LCE) of the cement paste around the aggregates themselves. The LCE may vary considerably within the concrete sample and it is related to the relative distance between the aggregates, their stiffness and their dimensions.

- For these reasons a specific plasto-damage formulation for the concrete matrix has been carried out to evaluate the stress distribution in a mesoscale approach.

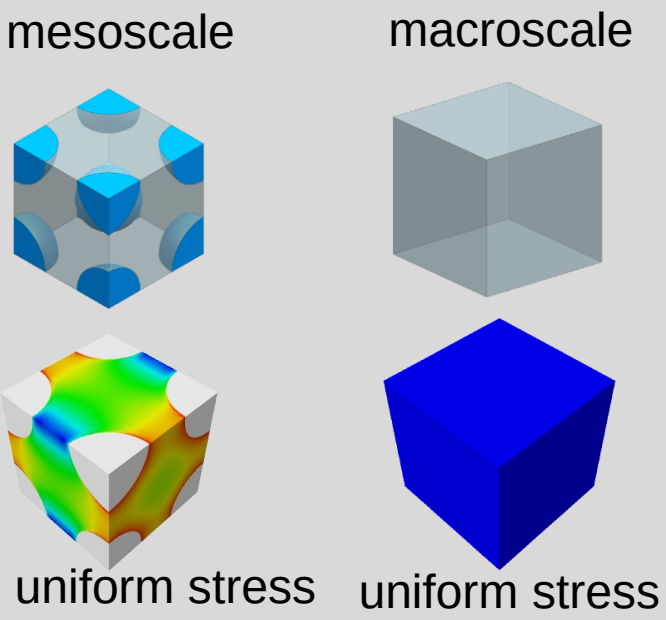

CONSTITUTIVE MODEL

EAF SLAG AGGREGATES CONSTITUTIVE MODEL

Elasto-plastic constitutive behaviour based on uniaxial experimental tests on slags samples having different degrees of porosity

CEMENT MATRIX CONSTITUTIVE MODEL

Elasto-plastic-damaged constitutive behaviour

Three-Invariants Elasto Plastic Model

The yield function can be written as [1,2]:

$$f_p = 1.5\left(\frac{\rho}{f_c}\right)^2 + q_h(k)\frac{m}{f_c}\left[\frac{\rho}{\sqrt{6}}r(\vartheta,\mathrm{e}) + \frac{\xi}{\sqrt{3}}\right] - q_h(k)q_s(k) \le 0$$

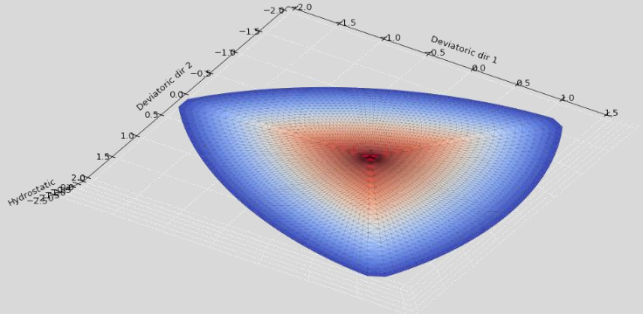

Yield surface with e=0.52

where k is the equivalent strain (plastic volumetric strain) and r is an elliptic function describing the cone roundness

e = eccentricity parameter [0.5÷1.0]

m is the cohesion parameter defined as: $m = 3\dfrac{f_c^2 - f_t^2}{f_c f_t}\dfrac{e}{e+1}$

$q(k) = q_h(k)q_s(k)$ is the plastic hardening softening function related to the material characteristics

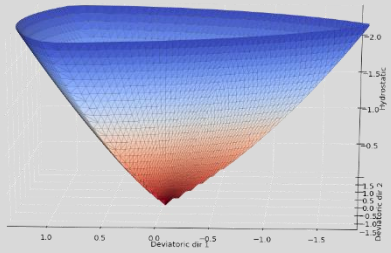

[1] Menetrey P., Willam KJ., ACI Struct J (1995);
[2] Mazzucco, G., Xotta, G., Pomaro, B., Salomoni, V.A. and Faleschini, F. Comp. Part B (2018)

CEMENT MATRIX CONSTITUTIVE MODEL

Three-Invariants Elasto Plastic Model *(contd)*

Hardening function $q_h(k) = q_{h0} + (1 - q_{h0})\sqrt{1 - \left(\frac{k_{1D} - k}{k_{1D}}\right)^2}$

Softening function $q_s(k) = \left[1 + \left(\frac{n_1 - 1}{n_2 - 1}\right)^2\right]^{-2}$ $\left(n_1 = \frac{k}{k_{1D}} \;;\; n_2 = \frac{(k_{1D} + t)}{k_{1D}}\right)$

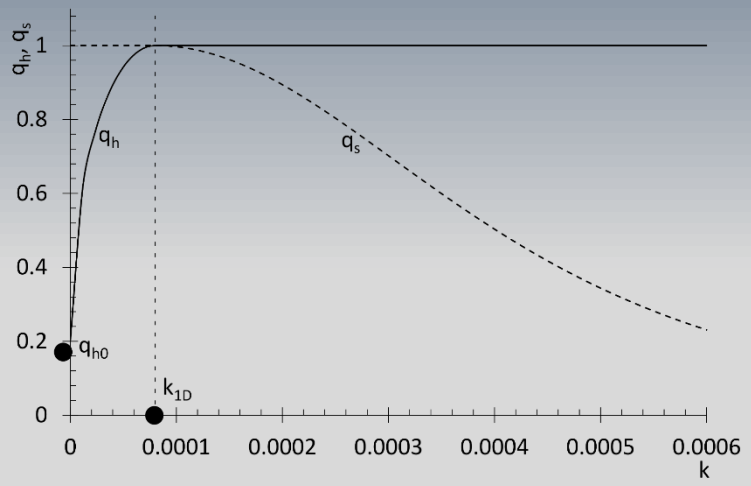

q_{h0} is the initial hardening parameter; k_{1D} is the plastic volumetric strain at the peak of the 1D curve and t is the softening function slope

A non-associated flow rule is considered, where the plastic potential g_p is so defined [1]

$$g_p = -g_A\left(\frac{\rho}{f_c(q_h q_s)^{1/2}}\right)^2 - g_B\left(\frac{\rho}{f_c(q_h q_s)^{1/2}}\right) + \frac{\xi}{f_c(q_h q_s)^{1/2}}$$

where g_A and g_B are material parameters related to the confinement effect

$$\dot{\varepsilon}_{ij}^p = \dot{\lambda}\frac{\partial g_p}{\partial \sigma_{ij}} \qquad \dot{k}(\boldsymbol{\varepsilon}^p) = \delta_{ij}\dot{\varepsilon}_{ij}^p = \dot{\lambda}\frac{\partial g_p}{\partial \sigma_{ij}}$$

δ_{ij} is the Kronecker tensor; λ is the plastic multiplier

[1] Grassl P., Karin L.n, Kent G., Int. J. of Sol. and Struc., (2002).

CEMENT MATRIX CONSTITUTIVE MODEL

Scalar Isotropic Damage Model

An isotropic damage model is taken into account [1]

$$\varepsilon_t = \frac{I_\varepsilon}{2(1-2\nu)} + \frac{\sqrt{J_\varepsilon}}{2(1+\nu)}$$

$$\varepsilon_c = \frac{I_\varepsilon}{5(1-2\nu)} + \frac{6\sqrt{J_\varepsilon}}{5(1+\nu)}$$

equivalent strains in tension and compression

$f_{d,t} = \varepsilon_t - Y_t \le 0$; $f_{d,c} = \varepsilon_c - Y_c \le 0$ loading surfaces in tension and compression

$$Y_t = \max\left[\varepsilon_{0t}, \varepsilon_t\right] \; ; \; Y_c = \max\left[\varepsilon_{0c}, \varepsilon_c\right]$$

$$Y = rY_t + (1-r)CY_c$$

where C is the confinement coeff:

$$C = \begin{cases} 1 & if \;\; r > 0 \\ \dfrac{\sum\langle\varepsilon_i\rangle}{\sum\langle\varepsilon_{0i}\rangle} & if \;\; r = 0 \end{cases}$$

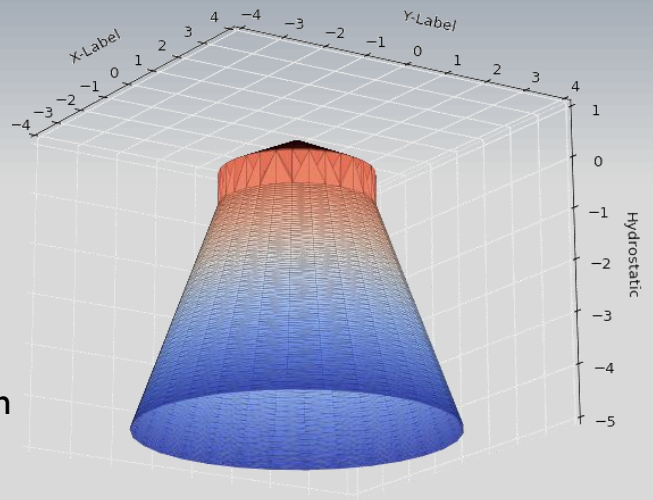

Failure surface

$$r = \frac{\sum\langle\bar{\sigma}_i\rangle}{\sum|\bar{\sigma}_i|}$$

triaxial parameter

$$\omega = 1 - \frac{(1-A^\omega)Y_0}{Y} - A^\omega e^{\left[-B^\omega(Y-Y_0)\right]}$$

[1] Mazars J., Hamon F., Grange S., Mat. and Struc., (2015).

CEMENT MATRIX CONSTITUTIVE MODEL

The damage-plastic model [1] is based on effective stresses

$$\boldsymbol{\sigma}_n^{pd} = \left(1-\omega_n\right)\bar{\boldsymbol{\sigma}}$$

The sequence to combine the damage model into the plastic field is:

- Elastic Trial condition
- Return mapping to plastic surface
- Damage correction

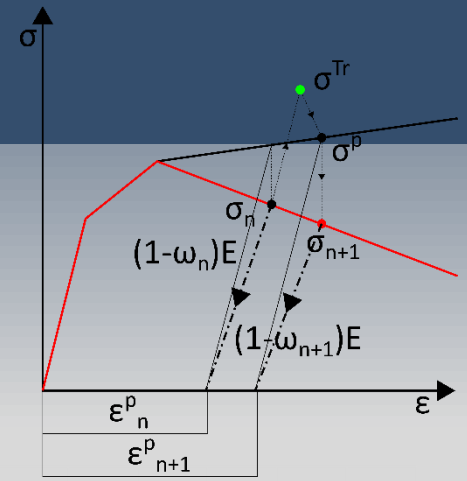

Constitutive Tangent Tensor

$$\mathbf{C}_n^{pd} = \left(1-\omega_n\right)\mathbf{R}\left(\mathbf{I}-\frac{\mathbf{g}_\sigma\mathbf{f}_\sigma\mathbf{R}}{\mathbf{f}_\sigma\mathbf{R}\mathbf{g}_\sigma - H\left(k\right)}\right)-\frac{\partial\omega_n}{\partial\dot{\boldsymbol{\varepsilon}}_n^p}\partial\bar{\boldsymbol{\sigma}}$$

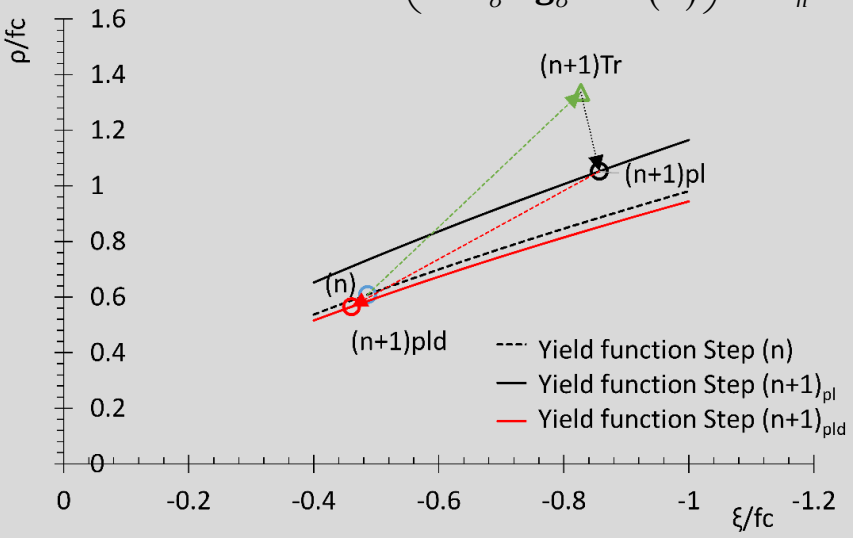

Stress path

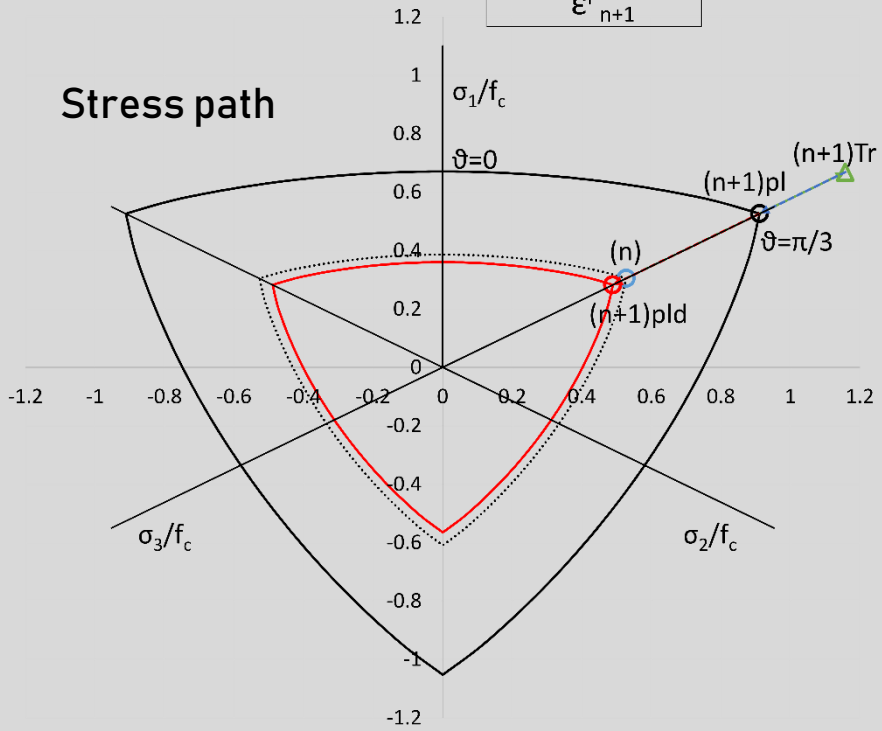

[1] Mazzucco, G., Xotta, G., Pomaro, B., Salomoni, V.A. and Faleschini, F. Comp. Part B (2018)

Non-Local Algorithm

- Using the elastoplastic or plasto-damage theory during the softening behaviour the solutions analysis is mesh dependent.
- Basically this is because the governing field equations of a continuum model looses ellipticity [1].
- The localized plastic strain width is related to the heterogeneous material microstructure and it can be correctly predicted by an intrinsic parameter with the dimension of length *l* [2]:

$$\bar{\varepsilon}^{eq}\left(\mathbf{x}_i\right)=\frac{1}{V_r}\int_V \alpha\left(\mathbf{x}_i,\mathbf{x}\right)\varepsilon^{eq}\partial V \qquad V_r=\int_V \alpha\left(\mathbf{x}_i,\mathbf{x}\right)\partial V$$

ε^{eq}	*Equivalent plastic strain*
$\bar{\varepsilon}^{eq}$	*Non-local Equivalent plastic strain*
$\alpha\left(\mathbf{x}_i,\mathbf{x}\right)$	*Non-local weigh*

- The volume integral in finite element implementation can be evaluated using the parent element [3]

$$\int_V \alpha\left(\mathbf{x}_i,\mathbf{x}\right)\varepsilon^{eq}\partial V=\int_{-1}^{1}\int_{-1}^{1}\int_{-1}^{1}\alpha\left(\mathbf{x}_i,\mathbf{x}\right)\varepsilon^{eq}\det\mathbf{J}\partial\xi\partial\rho\partial\zeta$$

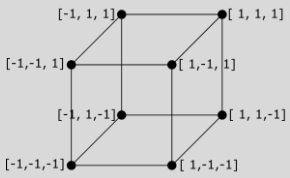

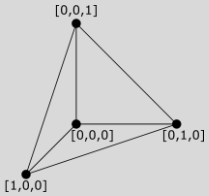

$$\bar{\varepsilon}^{eq}\left(\mathbf{x}_i\right)=\frac{\sum_{e=1}^{n}\sum_{ip=1}^{m}\omega_{ip}\alpha\left(\mathbf{x}_i,\mathbf{x}\right)\det\mathbf{J}_{ip}^{e}\varepsilon^{eq}\left(\mathbf{x}_{ip}\right)}{\sum_{e=1}^{n}\sum_{ip=1}^{m}\omega_{ip}\alpha\left(\mathbf{x}_i,\mathbf{x}\right)\det\mathbf{J}_{ip}^{e}}$$

[1] De Borst R. "Simulation of strain localization: a reappraisal of the Cosserat continuum",(1991).
[2] Bazant Z. et al (2003), "Non-local yield limit degradation.
[3] Lazari M. et al, (2015), "Local and non-local elasto-viscoplasticity in strain localization analysis of multiphase geomaterials".

SLAG MECHANICAL CHARACTERIZATION

3D LASER SCANNER

Acquisition of the exact shape of the inclusions added to the concrete mix design

Each inclusion has been coloured to increase the scanner precision.

3D laser scanner output
CLOUD POINTS

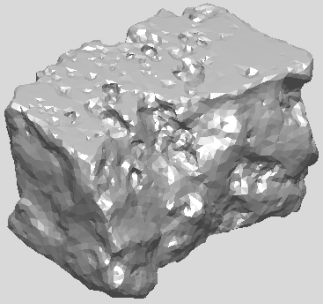

SCANNING

Graphic elaboration in surfaces (tesselation) and realization of 3D geometry

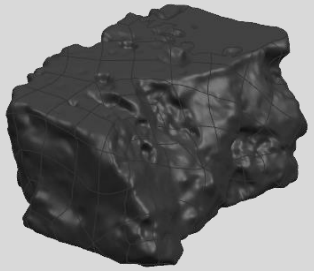

3D GEOMETRY

EXPERIMENTAL CAMPAIGN – EAF SLAG AGGREGATES

Uniaxial experimental tests performed on EAF slags samples characterized by different levels of macro porosities

(as a result of their origin, slags will be more porous if coming from solidified material on the surface and denser if coming from solidified material in depth)

A common elasto-plastic behavior for the aggregates is assumed in the numerical analyses, equal to an average value of what has been obtained in the different experimental tests (see avg curve ⇨)

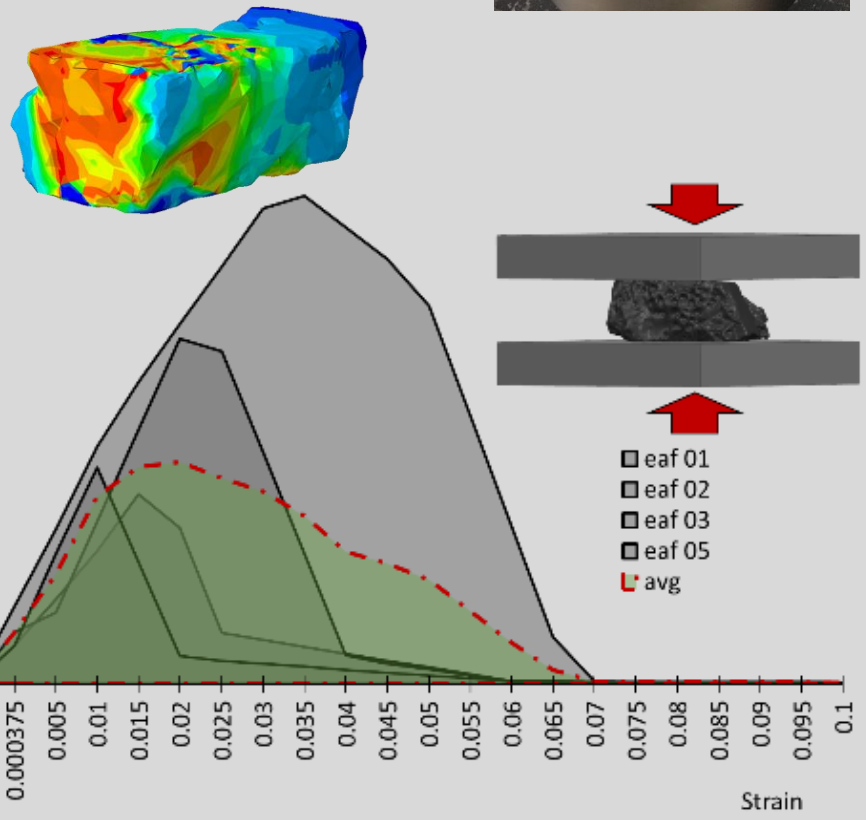

RANDOM DISTRIBUTION

Ellipsoids intersection check [1]

During the aggregate collocation procedure, the ellipsoids should not intersect.
Taken two ellipsoids E_0 and E_1 defined with two ellipsoid matrices $\mathbf{M}_0$ and $\mathbf{M}_1$ as:

$$\mathbf{x}^T\mathbf{M}_0\mathbf{x} \le 0 \;\; ; \;\; \mathbf{x}^T\mathbf{M}_1\mathbf{x} \le 0$$

The intersection can be evaluated based on the eigenvalues of the system:

$$\det\left[\mathbf{M}_0\left(\lambda I - \mathbf{M}_0^{-1}\mathbf{M}_1\right)\right] = 0 \qquad \begin{cases} if \quad \lambda_i > 0 \quad \in R^3 \\ if \quad \lambda_i < 0 \quad \in R^3 \\ if \quad \lambda_i \quad\quad \in C^3 \end{cases}$$

the two ellipsoids penetrate
the two ellipsoids are detached
the two ellipsoids intersect

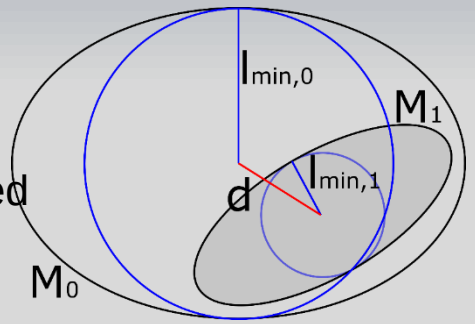

If the ellipsoids are intersecting a dislocation procedure is activated:

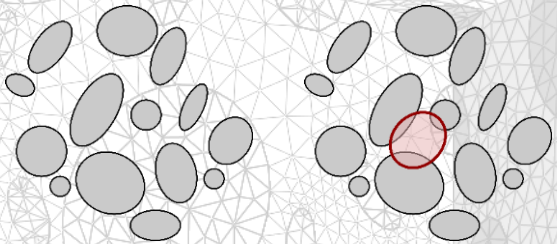

[1] initial configuration

[2] a new trial inclusion (I^{tr}) is added assuming a random position into the sample space

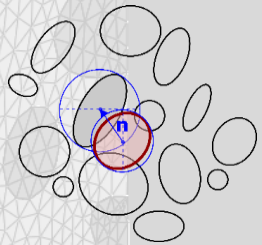

[3] if the interference is found a shift of the initial configuration is imposed to increase de void space and so positioning the I^{tr}

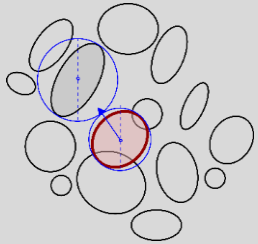

[4] the shift direction vector is defined considering the distance between the centres of the two circumscribed spheres. The displacement magnitude is obtained by the tangency condition.

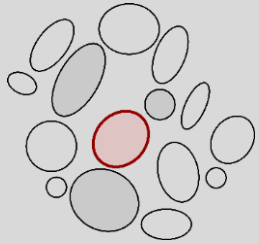

[5] this movement can be validated if the shifted inclusion does not touch the nearby inclusions.

[1] Mazzucco G., Pomaro B., Salomoni V., Majorana C. Con. & Buil. Mat. (2018)

RANDOM DISTRIBUTION

Concrete with gravel aggregates

Grading curve [1]

Gravel	22%	Coarse Ballast	23%	Fine Ballast	10%
Sieves	*Passing*	*Sieves*	*Passing*	*Sieves*	*Passing*
31.5	100.00	31.50	100.00	31.50	100.00
25.00	100.00	25.00	100.00	25.00	100.00
20.00	71.62	20.00	100.00	20.00	100.00
16.00	13.91	16.00	96.92	16.00	100.00
12.50	0.41	12.50	67.52	12.50	100.00
8.00	0.00	8.00	2.56	8.00	99.81
4.00	0.00	4.00	0.17	4.00	42.94
2.00	0.00	2.00	0.00	2.00	7.89
1.00	0.00	1.00	0.00	1.00	0.97
0.50	0.00	0.50	0.00	0.50	0.19
0.25	0.00	0.25	0.00	0.25	0.00
0.12	0.00	0.13	0.00	0.13	0.00
0.06	0.00	0.06	0.00	0.06	0.00
0.00	0.00	0.00	0.00	0.00	0.00

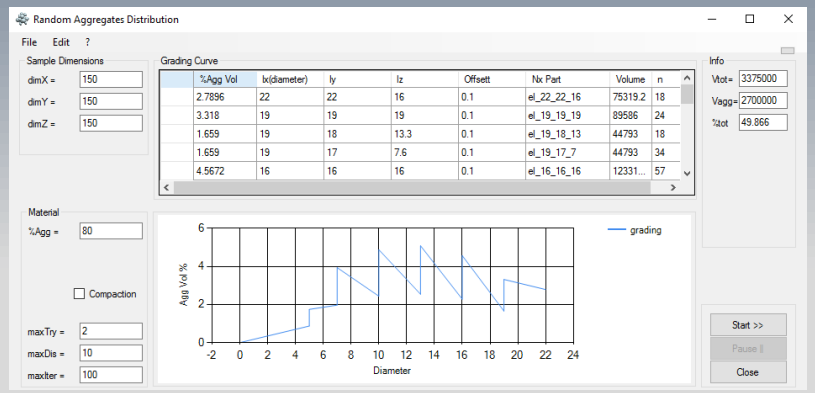

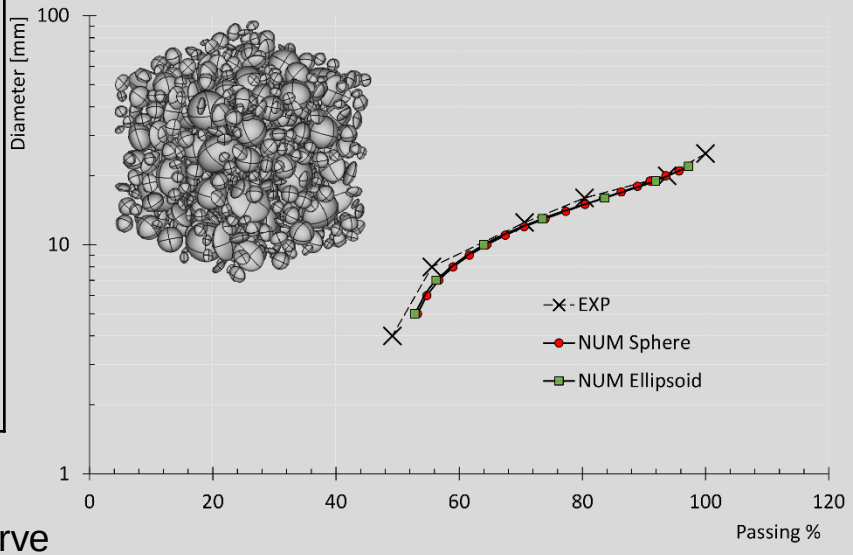

3% of average error between real and numerical grading curve

SOLID MODELS

To strictly compare experimental and numerical results, solid models are created with the support of advanced techniques of measurement and detection

3D INDUSTRIAL COMPUTED TOMOGRAPHY (CT)

Exact reproduction of the tested specimens; the geometry of the inclusions and their placement

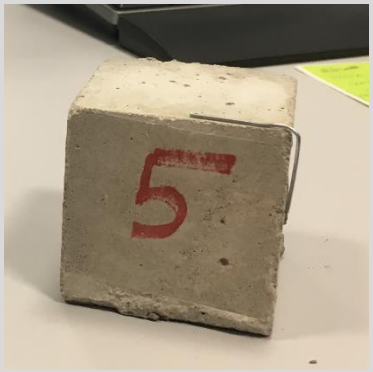

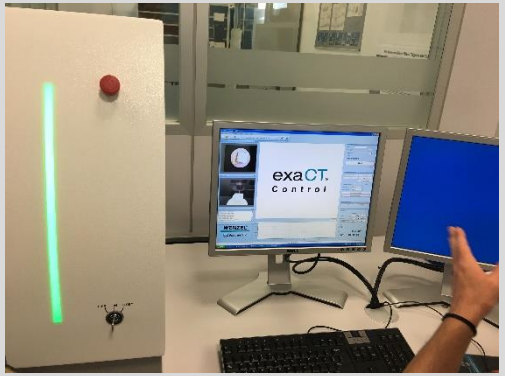

CT output
CLOUD POINTS

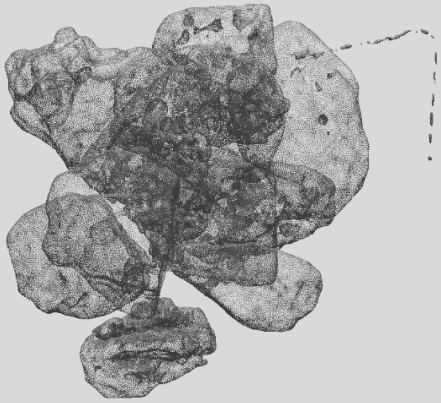

Graphic elaboration in surfaces (tesselation) and realization of 3D geometry

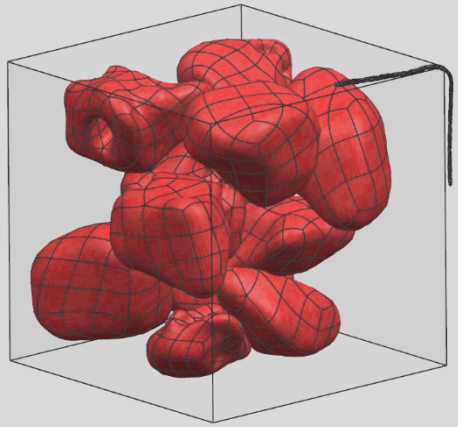

3D GEOMETRY

EXPERIMENTAL CAMPAIGN - CONCRETE SPECIMENS

Uniaxial compression tests on three cubic samples made of 100% EAF aggregates,

Size of the samples: 50x50x50 mm^3

Mix Design:
w/c = 0.5
a/c ≈ 0.33
CEM II 32.5R

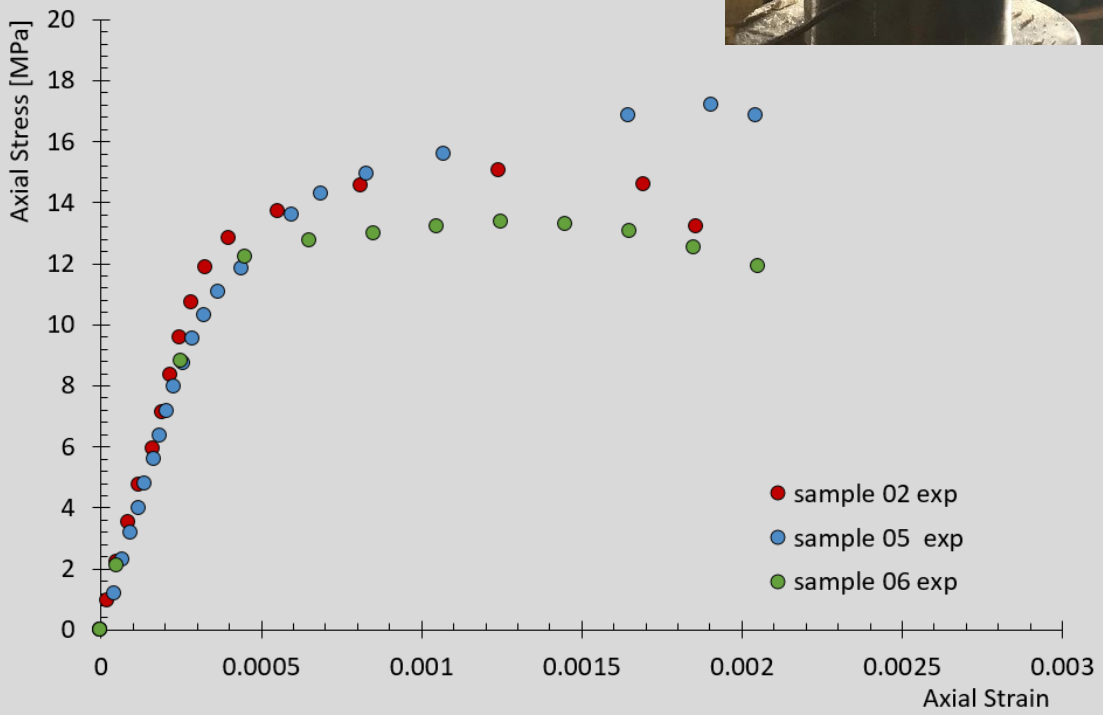

NUMERICAL MODELS

- Development of three numerical models at the meso-scale level, in agreement with the experimental tests.
- Same shape and placement of slag inclusions, for real samples and numerical models, using 3D computed tomography

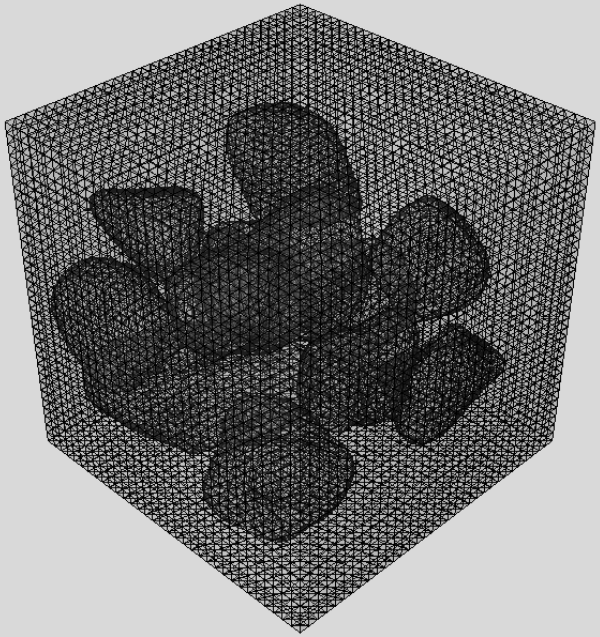

SAMPLE 02

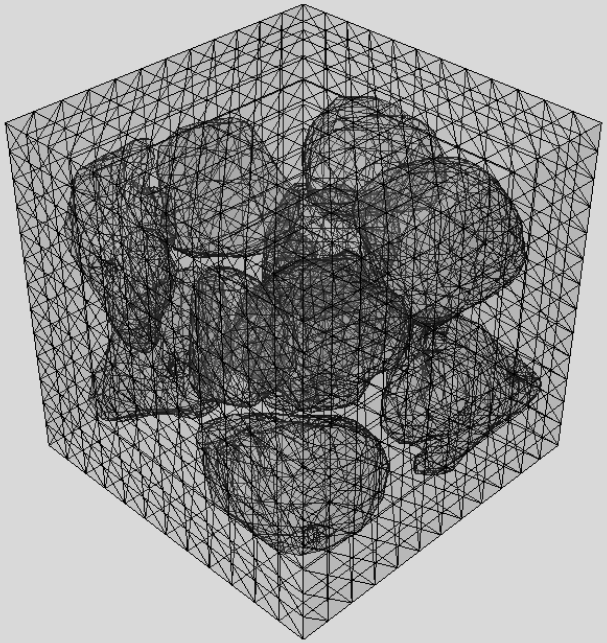

SAMPLE 05

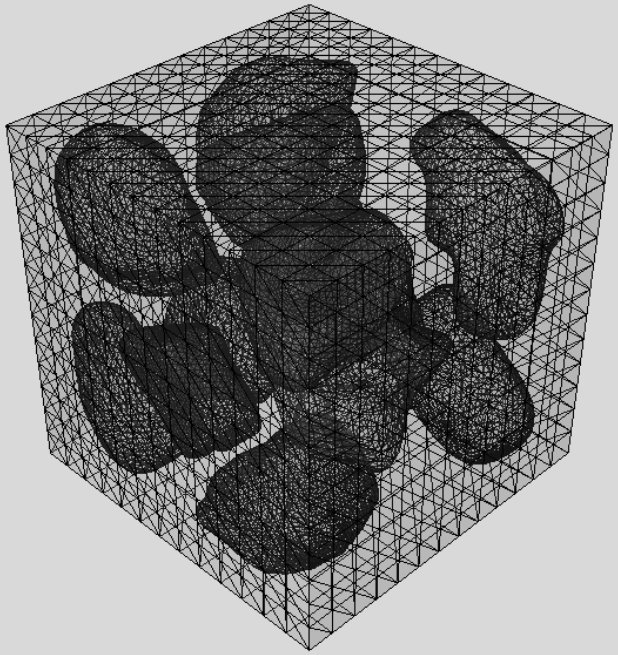

SAMPLE 06

NUMERICAL MODELS

CEMENT MATRIX
elasto-plasto-damaged material

PLASTICITY		
E	29450	MPa
ν	0.15	
f_c	32	MPa
f_t	2.8	MPa
e	0.52	
t	0.001	
k_{1D}	0.06	
q_{h0}	0.1	
g_A	-21.22	
g_B	-31.46	

DAMAGE	
k_{dt}	0.0006
k_{dc}	0.0022
A_t	0.8
B_t	800
A_c	0.5
B_c	100

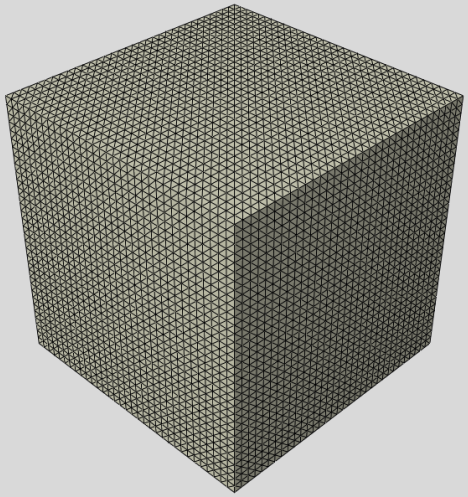

EAF ggregates
Elasto-plastic material

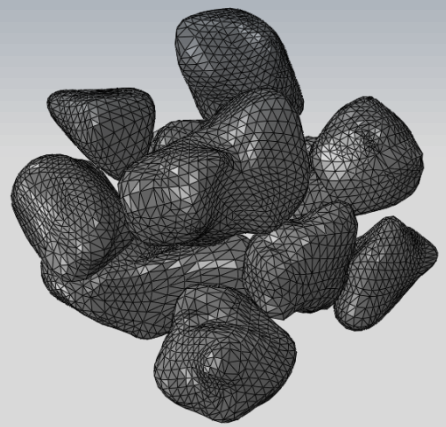

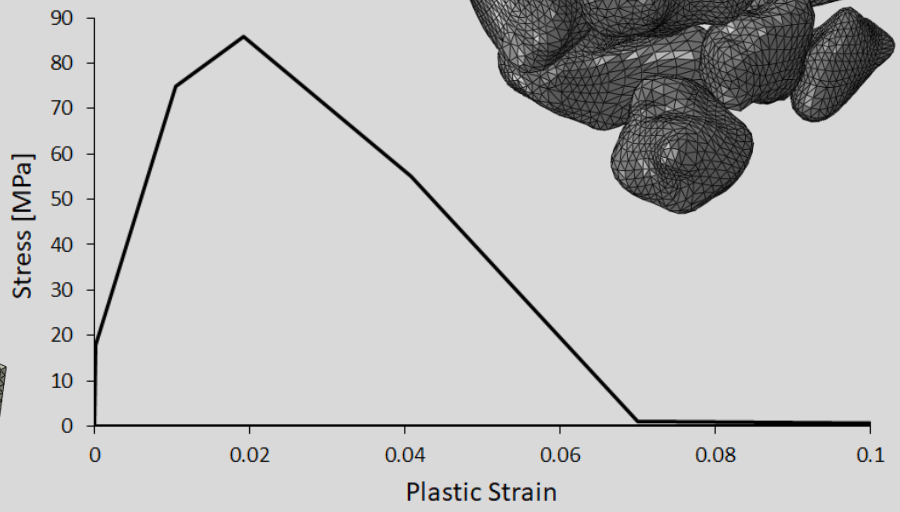

E	71250	MPa
ν	0.15	

NUMERICAL MODELS

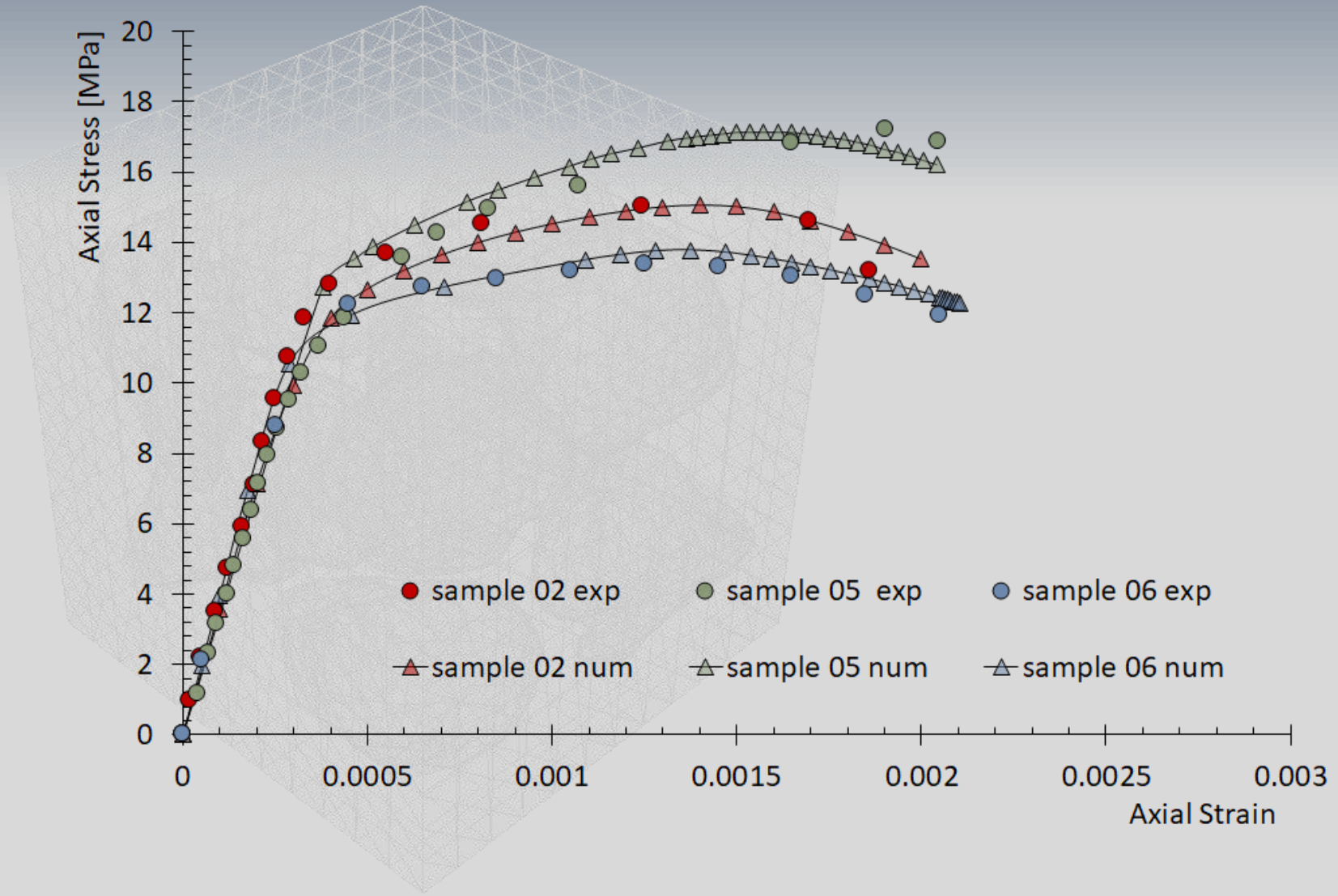

NUMERICAL MODELS

DAMAGE EVOLUTION

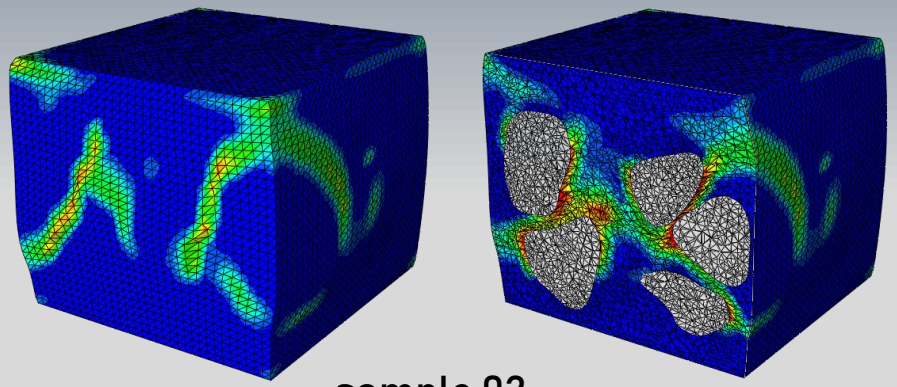

sample 02

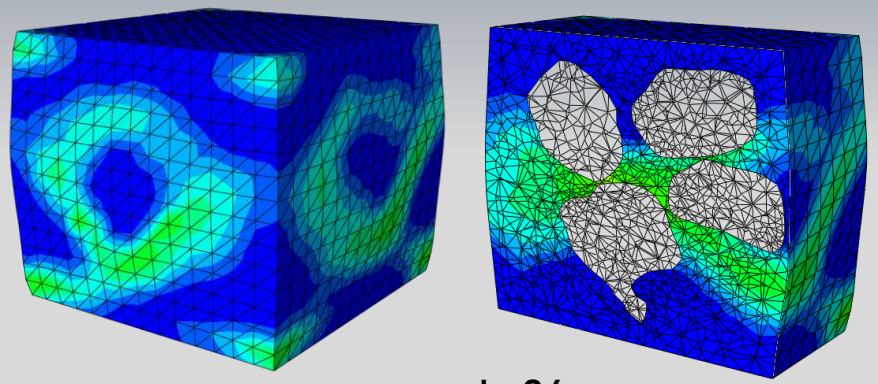

sample 06

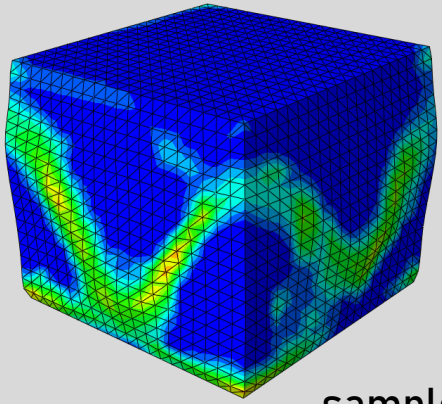

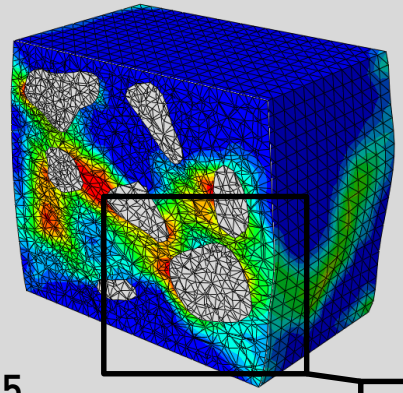

sample 05

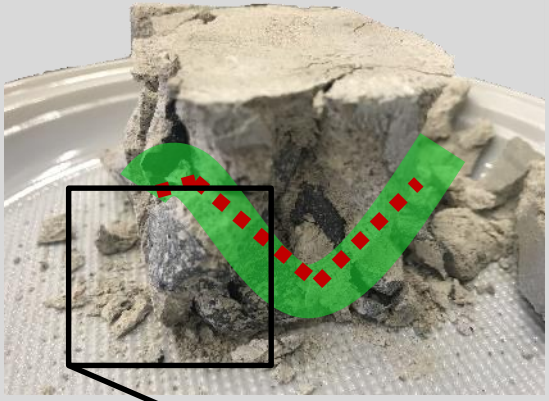

Aggregate expulsion
from the sample edge

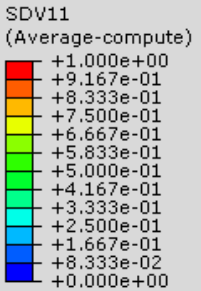

CONCLUSIONS

- The mechanical behaviour of concrete made with EAF recycled aggregates has been investigated in this work adopting a meso-scale approach.
- 3D advanced measurement techniques have been adopted to exactly reproduce the tested specimens and the EAF inclusions
- An elasto-plasto-damaged constitutive model has been developed and adopted to describe cement matrix while slag aggregates are characterized by an experimental based elasto-plastic behaviour → local confinement effect between aggregates and cement paste is taken into account
- Comparisons between experimental evidences and numerical results have been reported, highlighting that the proposed approach is able to reproduce concrete behaviour under compression loads